Three-Dimensional Terrain Visualization on Personal Computers: An Application with Stereo SIR-B Images

R. Welch and *D. Papacharalampos*
Center for Remote Sensing and Mapping Science (CRMS), Department of Geography, The University of Georgia, Athens, GA 30602

ABSTRACT: A low-cost personal computer and image processing/mapping software package were employed to derive terrain elevations from Shuttle Imaging Radar-B (SIR-B) stereo image data in digital formats, and to create three-dimensional (3D) perspective views of the rugged Mt. Shasta area in northern California. Elevation errors of less than ±65 m were achieved using automatic stereocorrelation techniques and a linear DEM calibration approach. It is anticipated that future radargrammetric mapping and terrain visualization studies can be conducted using digital stereo radar images in a PC-based workstation environment. This will greatly facilitate utilization of radar images for studies of the perennial cloud-covered areas of the world.

INTRODUCTION

SYNTHETIC APERTURE RADAR (SAR) images have proved useful for a variety of landform and land-use analysis tasks. They also have been employed to derive terrain elevations (Ford *et al.*, 1986; Leberl *et al.*, 1986a). However, the computation of *Z*-coordinates from stereo SAR data in digital formats is a difficult task, even with large, powerful computers (Ramapriyan *et al.*, 1986). Factors that influence the derivation of terrain elevations include inherent noise, a relatively narrow range of useful intensity values, comparatively poor spatial resolution, layover caused by terrain relief, and variable geometric characteristics introduced during acquisition. These problems are well-known and were encountered in the present study of Shuttle Imaging Radar-B (SIR-B) data of Mt. Shasta in northern California (Figure 1).

Previous mapping studies have been conducted with SIR-B data of Mt. Shasta, including those by Leberl *et al.* (1986b) and Simard *et al.* (1986), both of whom employed stereo-pairs recorded at incidence angles of 29 and 53 degrees. The former study utilized image processing techniques to generate optimized film transparencies from the digital SIR-B data. These film images were then inserted in an analytical stereoplotter controlled by specially tailored software to produce spot heights and a contour plot at an interval of 200 m. The root-mean-square error (RMSE) of spot heights ranged from ±53 m to ±178 m. Simard *et al.* (1986), on the other hand, employed automated stereocorrelation techniques to generate elevations and orthoimages from the digital SIR-B stereo images. However, correlation success was limited to about 33 percent, and comparisons with map data revealed the stereocorrelation produced a root-mean-square difference of about ±100 m between map and image-derived *Z*-coordinate values. While the above studies document the possibilities for producing topographic information from the stereo SIR-B data, and for generating maps, orthoimages, and 3D displays, they also indicate the problems of working with SAR images in digital formats.

The objective of this study is to expand the previous work by demonstrating the heretofore unrealized possibilities for generating topographic information from digital SAR images using automated stereocorrelation and terrain visualization techniques with personal computers (Welch and Papacharalampos, 1990). At the time this study was conducted, automatic stereocorrelation of digital SAR data had not been demonstrated on small computers. Furthermore, Earth scientists seldom have access to details about SAR sensor geometry that will be of use in terrain mapping. Consequently, an effort was made to develop correlation techniques in combination with a simplified computational approach for deriving terrain elevations that can be used by geomorphologists, geologists, and map makers.

FIG. 1. Study area is centered on Mt. Shasta in northern California.

A software package, the Desktop Mapping System (DMS)™, developed to create planimetric, topographic, and thematic map products from digital images has been employed for this purpose (Welch, 1989). The DMS software is designed to permit low-cost, effective image processing and 3D terrain mapping on IBM compatible personal computers (Welch, 1990). It provides a rigorous 3D mapping capability when employed with SPOT stereo images, and is well suited for use with image data recorded by a variety of sensor systems.

All data processing in this study was undertaken on a Dell 325 personal computer equipped with Intel 80386 and 80387 microprocessors operating at 25 MHz. The memory system included 4 Mbytes of RAM and a 320 Mbyte hard disk. An IBM 8514/A compatible display adapter and monitor provided 256 colors at 1024-pixel by 768-line resolution. The DMS software package running under MS-DOS 4.0 incorporated all necessary routines for rectification, registration, stereocorrelation, and three-dimensional display.

PHOTOGRAMMETRIC ENGINEERING & REMOTE SENSING,
Vol. 58, No. 1, January 1992, pp. 71–75.

0099-1112/92/5801–71$03.00/0

STUDY AREA AND STEREO SIR-B DATA SETS

The study area is centered on Mt. Shasta, California (41° 25′ N latitude and 122° 10′ W longitude) and covers approximately 700 km². Elevations range from about 800 m to more than 4300 m above sea level.

Available data sets included three images with 25-m pixel resolution recorded at incidence angles of 29.7, 53.8, and 63.8 degrees during the SIR-B mission of October 1984 (Cimino *et al.*, 1988), and two US Geological Survey 1:62,500 scale topographic maps. As in the previous studies by Leberl *et al.* (1986b) and Simard *et al.* (1986), the images with incidence angles of 29.7 (left) and 53.8 (right) degrees were selected for analysis. These images provide the most complete coverage of Mt. Shasta and exhibit the best visual stereo perception of relief (Figure 2).

DEM GENERATION AND DISPLAY

The steps required to derive a regular grid of terrain elevations from digital satellite image data by automated stereocorrelation techniques were previously described by Ehlers and Welch (1987). These have been modified to accommodate the SIR-B digital images. This modified approach includes preprocessing, image registration/rectification, automatic stereocorrelation, DEM calibration, and display and output product generation as shown in Figure 3. Each of these steps is described below.

PREPROCESSING

A series of initial tests with the rather noisy SIR-B data sets revealed that a pixel resolution of 25 m was too fine to permit reliable correlation over an area having relief in excess of 3500 m. To minimize noise, 2 by 2 blocks of pixels were aggregated to create images of 50-m resolution which in turn were smoothed with a 3 by 3 average filter. Finally, the images were rotated 90 degrees to ensure that parallaxes were aligned in the x-direction.

IMAGE REGISTRATION

Stereocorrelation techniques assume that any differences between the left and right images are caused by relief displacement. Therefore, it was necessary to register the right image to the left (reference) image using well-distributed image control points common to both images and lying at approximately the same elevation. Although a minimum of three points are required for registration, a total of six image control points with an average elevation of 1085 m were selected for this study. The x, y image coordinates of these points were measured to subpixel accuracy, and coefficients were computed to transform right image space coordinates to left image space using a least-squares polynomial solution. The RMSE of the registration was about ± 32 m (± 0.65 pixels). By registering the images to common points at an elevation that establishes a local vertical da-

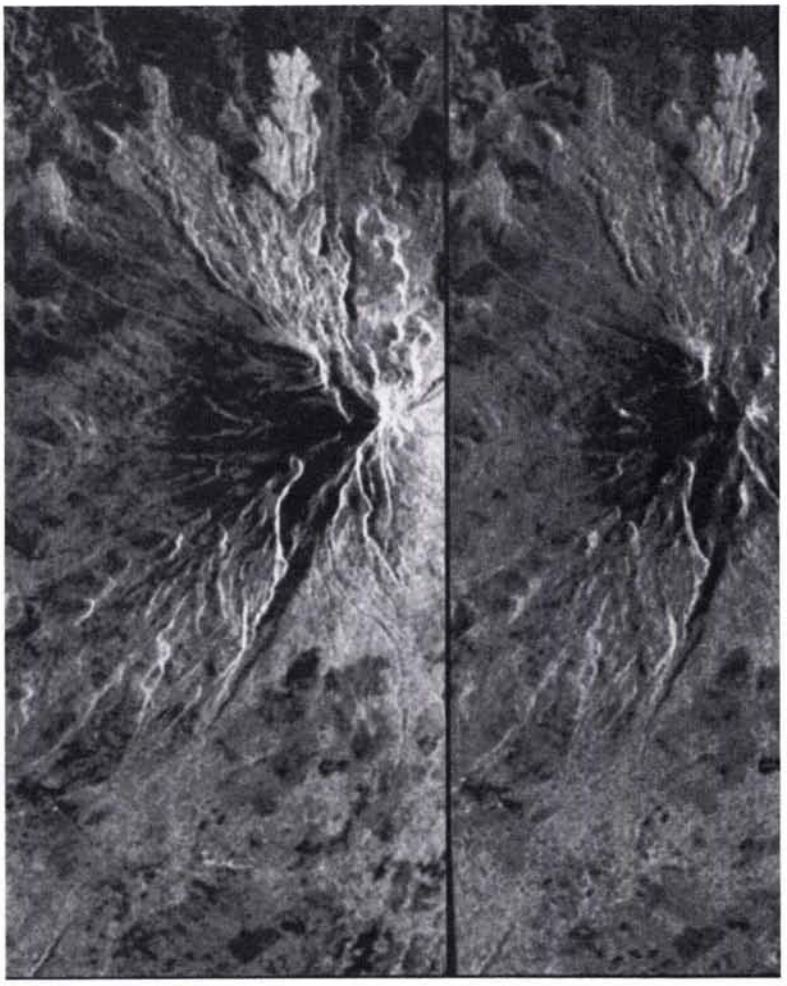

FIG. 2. Stereo SIR-B images of Mt. Shasta. Note the shading and relief displacement, both of which can hinder stereo perception and correlation.

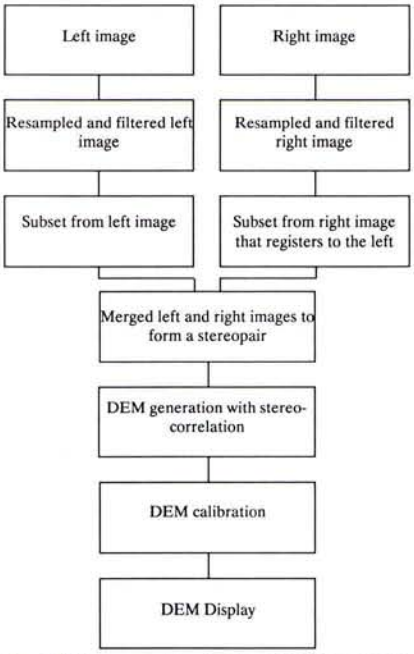

FIG. 3. Steps used to derive a DEM from SIR-B image data sets.

tum, y-parallax is minimized and x-parallax is zero at the datum elevation.

After registration, a 50-m resolution 346-pixel by 768-line stereo subset of the Mt. Shasta area was extracted for stereocorrelation. This subset has no y-parallax and can be viewed in stereo by displaying the left image in red and the right image in green and blue. Enhancement techniques such as histogram equalization were employed to improve the stereo perception of relief.

STEREOCORRELATION

Stereocorrelation requires matching pixel locations in the left (L) and right (R) images of the stereopair. As shown in Figure 4, this is accomplished by centering a correlation window on a pixel location (L_{xy}) in the left image and, assuming no relief displacement, defining a larger search window centered at the corresponding pixel location ($R_{x_o y_o}$) in the right image. The correlation window is then systematically moved to all pixel locations within the search window, and the correlation between the pixels in the left and right images is computed. The pixel location at which maximum correlation is recorded defines the match between L_{xy} and R_{xy}. A difference in pixel location in the x-direction between R_{xy} and $R_{x_o y_o}$ is the parallax difference (Δp). The Δp value is proportional to the elevation difference (Δh) between the measured point and the local vertical datum established by the control points used to register the stereopair.

The reliability of the matching process can be increased by accepting only points with a statistically significant correlation, and interpolating the measured location to subpixel level. If the anticipated minimum and maximum elevations in the area are known, then limits can be placed in the search process to improve performance. This procedure can be repeated for all pixel locations, or for pixels spaced at a regular grid interval.

The stereocorrelation option of the DMS permits definition of the grid (or sampling) interval and the size of both correlation and search windows. By increasing the interval or decreasing window sizes, significant increases in correlation speed can be realized. The optimum correlation window will be a function

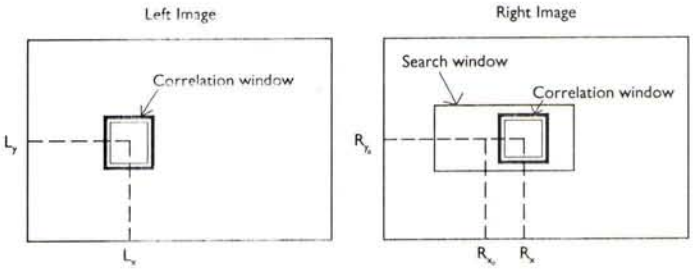

FIG. 4. Generalized stereocorrelation point matching procedure.

of the image content and the signal-to-noise ratio of the stereopair. Its size may vary from one stereopair to another.

In this study, experiments were conducted with correlation windows ranging from 3 by 3 to 17 by 17 pixels. Optimum results were obtained with a 13 by 13 correlation window. A relative DEM of Δp values (in pixel units) at an interval of 100 m (2 pixels) was calculated in less than 75 minutes with 76 percent of the points correlated successfully. Outliers in the Δp values such as spikes were corrected using a modified median filter with appropriate thresholds. Finally, this relative DEM was smoothed with a 3 by 3 average filter to reduce high frequency noise. Due to extreme relief and distortions, the top of Mt. Shasta (above 2500 m) was not correlated.

DEM CALIBRATION

It was necessary to transform the Δp values to a true DEM of Z-values in ground units (metres). Before undertaking this transformation, however, relief displacements were removed from the left image of the stereopair by shifting each pixel by the Δp component for that location. Although only three ground control points (GCPs) are needed, eight GCPs were employed to establish rectification coefficients required to fit the "relief corrected" image to the map. These coefficients also allow the planimetric (map) coordinates to be instantly determined for any relative DEM location, thus enabling accuracy evaluations (as described below) to be conducted once the Δp values have been transformed to ground elevations.

Conversion of the Δp values to yield a true DEM in ground units was accomplished using a calibration technique that involved constructing a terrain profile from 13 map points progressively increasing in elevation from 1200 m to 2000 m. By calculating a linear fit of the Δp values to the map elevations, the following equation was derived to transform Δp values to absolute ground elevations:

$$Z_i = 1075.2 + 50.3 * \Delta p_i$$

which may be generalized to

$$Z = a + b * \Delta p$$

where

- Z = the absolute ground elevation for a DEM cell at point i,
- a = ground elevation for the approximate vertical reference datum as established by the image control points selected to register the stereopair,
- b = scaling coefficient approximating the profile's slope,
- Δp = difference in x-parallax in pixels at point i.

It must be noted that only two points at representative minimum and maximum elevations for the topographic data set are needed to estimate the above coefficients. Of course, three or more points will increase the reliability of the transformation parameters. A direct comparison of map and image derived Z-coordinates for the terrain profile on which the calibration was

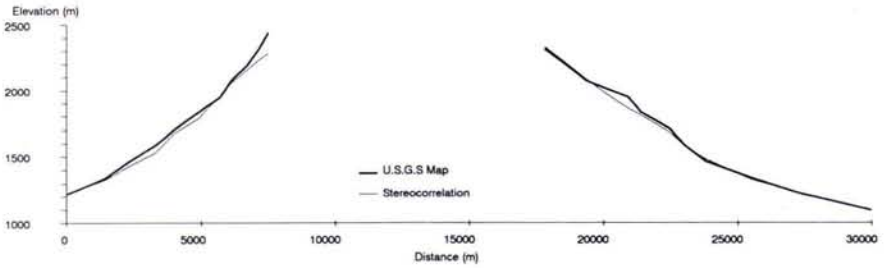

FIG. 5. Comparison of terrain profiles derived from the stereo SIR-B images and the USGS maps.

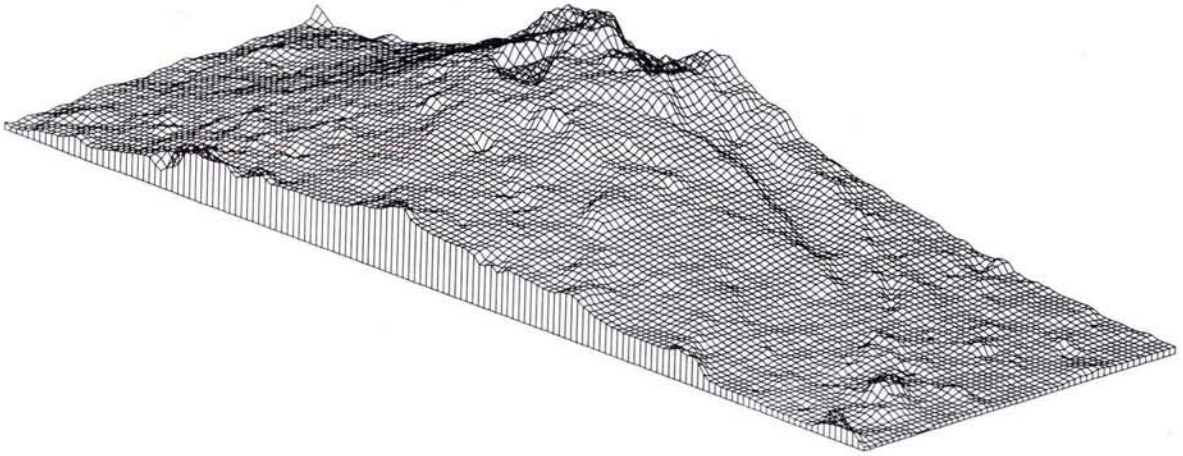

FIG. 6. Perspective wireframe display of the Mt. Shasta DEM.

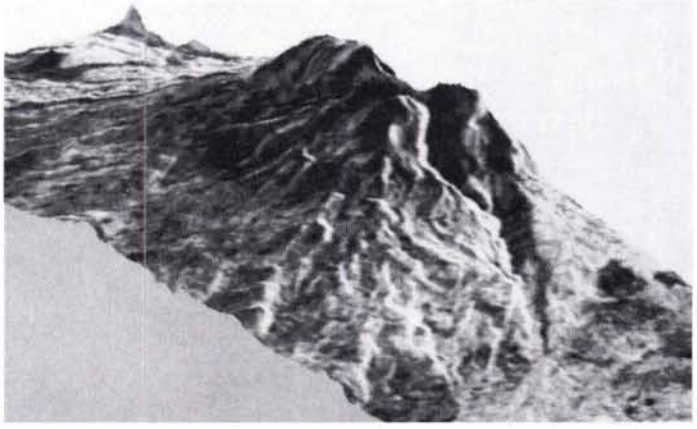

FIG. 7. The perspective wireframe draped with the SIR-B image pixel gray values.

based produced a root-mean-square difference of ±32 m. Application of the coefficients to other profiles (for which the terrain elevations were known) yielded root-mean-square differences in elevation of about ±40 m for areas of moderate relief, and ±65 m for areas of high relief (Figure 5). Variations in the differences between map- and image-derived values are to be expected, because the geometric parameters change with relief and the use of a linear equation to calculate Z-coordinates represents an approximate solution. Nevertheless, these techniques appear to yield elevation values of comparable accuracy to those determined by more rigorous methods. Leberl *et al.* (1986b), for example, list errors of ±53 m to ±178 m and Simard *et al.* (1986) obtained errors of ±100 m. Most importantly, they can be easily implemented by geologists, geographers, foresters, and other scientists wishing to develop a DEM from digital stereo radar data.

DEM Display and Output Products

Once a DEM has been established, it is possible to generate a perspective grid and to drape the SIR-B image values to create a realistic terrain visualization model (Figures 6 and 7). With the DMS software, viewing parameters such as azimuth, tilt, vertical exaggeration, and scale can be modified interactively as required. If desired, color-coded elevation, vector, and thematic geographic information system (GIS) files can be registered to the perspective. Because the left image has been corrected for relief displacement, a coordinate grid can be superimposed to produce an orthoimage map. These corrections also allow the radar data to be merged with Landsat or SPOT digital images using intensity-hue-saturation (IHS) techniques to create enhanced multispectral, multisensor data sets (Welch and Ehlers, 1988).

CONCLUSION

Terrain elevations can be determined from stereo digital radar image data sets using low-cost personal computers and image processing/mapping software such as the DMS which incorporates automatic stereocorrelation capabilities. Although the procedures used in this study for deriving absolute terrain elevations make no attempt to model sensor geometry, the accuracies of the Z-coordinates compare favorably with results produced in previous studies by more rigorous methods. More importantly, however, it has been demonstrated that stereo radar image data sets can be employed by scientists equipped with personal computers to derive terrain elevations by automated techniques and

to create orthoimage maps, 3D perspectives, and enhanced multiresolution, multisensor image products. Such capabilities lend themselves to a variety of mapping and GIS applications in the remote, poorly mapped areas of the world or in regions where cloud cover prevents obtaining photographic or electro-optical images of good quality.

ACKNOWLEDGMENTS

This study was conducted as part of the project, "Shuttle Imaging Radar-B (SIR-B) Data Analysis," funded by the California Institute of Technology Jet Propulsion Laboratory (JPL) under Contract No. 957516. The assistance of C. Elachi, D. Evans and M. Kobrick of JPL is greatly appreciated. The Desktop Mapping System (DMS)™ software package is marketed by R-WEL, Inc., P.O. Box 6206, Athens, GA 30604.

REFERENCES

Cimino, J.B., B. Holt, and A. Holmes Richardson, 1988. *The Shuttle Imaging Radar B (SIR-B) Experiment Report*, JPL Pub. 88-2, Jet Propulsion Laboratory, Pasadena, California.

Ehlers, M., and R. Welch, 1987. Stereocorrelation of Landsat TM Images, *Photogrammetric Engineering & Remote Sensing*, Vol. 53, No. 9, pp. 1231–1237.

Ford, J.P., J. B. Cimino, B. Holt, and M. R. Ruzek, 1986. *Shuttle Imaging Radar Views the Earth From Challenger: The SIR-B Experiment*, JPL Pub. 86-10, Jet Propulsion Laboratory, Pasadena, California.

Leberl, F.W., G. Domik, J. Raggam, J. B. Cimino, and M. Kobrick, 1986a. Multiple Incidence Angle SIR-B Experiment Over Argentina: Stereo-Radargrammetry Analysis, *IEEE Transactions on Geoscience and Remote Sensing*, Vol. GE-24, No. 4, pp. 482–491.

Leberl, F.W., G. Domik, J. Raggam, and M. Kobrick, 1986b. Radar Stereomapping Techniques and Application to SIR-B Images of Mt. Shasta, *IEEE Transactions on Geoscience and Remote Sensing*, Vol. GE-24, No. 4, pp. 473–481.

Ramapriyan, H.K., J. P. Strong, Y. Hung, and C. W. Murray, Jr., 1986. Automated Matching of Pairs of SIR-B Images for Elevation Mapping, *IEEE Transactions on Geoscience and Remote Sensing*, Vol. GE-24, No. 4, pp. 462–472.

Simard, R., F. Plourde, and T. Toutin, 1986. Digital Elevation Modeling with Stereo SIR-B Image Data, *Remote Sensing for Resources Development and Environmental Management, International Archives of Photogrammetry and Remote Sensing*, Vol. 26, Part 7/1, pp. 161–166.

Welch, R., 1989. Desktop Mapping with Personal Computers, *Photogrammetric Engineering & Remote Sensing*, Vol. 55, No. 11, pp. 1651–1662.

———, 1990. 3-D Terrain Modeling for GIS Applications, *GIS World*, Vol. 3, No. 5, pp. 26–30.

Welch, R., and M. Ehlers, 1988. Cartographic Feature Extraction with Integrated SIR-B and Landsat TM Images, *International Journal of Remote Sensing*, Vol. 9, No. 5, pp. 873–889.

Welch, R., and D. Papacharalampos, 1990. 3-D Computation and Display of Terrain Models from Stereo Imaging Radar Data, *Remote Sensing Science for the Nineties, Proceedings of the IEEE 10th Annual International Geoscience & Remote Sensing Symposium*, College Park, Maryland, Vol. 3, pp. 1967–1969.

Forthcoming Articles

Yue Hong Chou, Slope-Line Detection in a Vector-Based GIS.

Raymond L. Czaplewski, Misclassification Bias in Areal Estimates.

Claude R. Duguay and *Ellsworth F. LeDrew*, Estimating Surface Reflectance and Albedo from Landsat-5 Thematic Mapper over Rugged Terrain.

Peter F. Fisher, First Experiments in Viewshed Uncertainty: Simulating Fuzzy Viewsheds.

G. M. Foody, A Fuzzy Sets Approach to the Representation of Vegetation Continua from Remotely Sensed Data: An Example from Lowland Heath.

Steven E. Franklin and *Bradley A. Wilson*, A Three-Stage Classifier for Remote Sensing of Mountain Environments.

Clive S. Fraser, Photogrammetric Measurement to One Part in a Million.

Clive S. Fraser and *James A. Mallison*, Dimensional Characterization of a Large Aircraft Structure by Photogrammetry.

Peng Gong and *Philip J. Howarth*, Frequency-Based Contextual Classification and Gray-Level Vector Reduction for Land-Use Identification.

Christian Heipke, A Global Approach for Least-Squares Image Matching and Surface Reconstruction in Object Space.

Richard G. Lathrop, Jr., Landsat Thematic Mapper Monitoring of Turbid Inland Water Quality.

Donald L. Light, The New Camera Calibration System at the U.S. Geological Survey.

Ronald T. Marple and *Eugene S. Schweig, III*, Remote Sensing of Alluvial Terrain in a Humid, Tectonically Active Setting: The New Madrid Seismic Zone.

Fabio Maselli, Claudio Conese, Ljiljana Petkov, and *Raffaello Resti*, Inclusion of Prior Probabilities Derived from a Nonparametric Process into the Maximum-Likelihood Classifier.

Ram M. Narayanan, Steven E. Green, and *Dennis R. Alexander*, Soil Classification Using Mid-Infrared Off-Normal Active Differential Reflectance Characteristics.

Kurt Novak, Rectification of Digital Imagery.

Albert J. Peters, Bradley C. Reed, and *Donald C. Rundquist*, A Technique for Processing NOAA-AVHRR Data into a Geographically Referenced Image Map.

Kevin P. Price, David A. Pyke, and *Lloyd Mendes*, Shrub Dieback in a Semiarid Ecosystem: The Integration of Remote Sensing and Geographic Information Systems for Detecting Vegetation Change.

Omar H. Shemdin and *H. Minh Tran*, Measuring Short Surface Waves with Stereophotography.

Michael B. Smith and *Mitja Brilly*, Automated Grid Element Ordering for GIS-Based Overland Flow Modeling.

David M. Stoms, Frank W. Davis, and *Christopher B. Cogan*, Sensitivity of Wildlife Habitat Models to Uncertainties in GIS Data.

Khagendra Thapa and *John Bossler*, Accuracy of Spatial Data Used in Geographic Information Systems.

Thierry Toutin, Yves Carbonneau, and *Louiselle St-Laurent*, An Integrated Method to Rectify Airborne Radar Imagery Using DEM.

Paul M. Treitz, Philip J. Howarth, and *Peng Gong*, Application of Satellite and GIS Technologies for Land-Cover and Land-Use Mapping at the Rural-Urban Fringe: A Case Study.

William S. Warner and *Øystein Andersen*, Consequences of Enlarging Small-Format Imagery with a Color Copier.

Zhuoqiao Zeng and *Xibo Wang*, A General Solution of a Closed Form Space Resection.